

# Cloning, characterization, and mutational analysis of a highly active and stable L-arabinitol 4-dehydrogenase from *Neurospora crassa*

Ryan Sullivan · Huimin Zhao

Received: 7 August 2007 / Revised: 23 September 2007 / Accepted: 24 September 2007 / Published online: 16 October 2007  
© Springer-Verlag 2007

**Abstract** An NAD<sup>+</sup>-dependent L-arabinitol 4-dehydrogenase (LAD, EC 1.1.1.12) from *Neurospora crassa* was cloned and expressed in *Escherichia coli* and purified to homogeneity. The enzyme was a homotetramer and contained two Zn<sup>2+</sup> ions per subunit, displaying similar characteristics to medium-chain sorbitol dehydrogenases (SDHs). High enzymatic activity was observed for substrates L-arabinitol, adonitol, and xylitol and no activity for D-mannitol, D-arabinitol, or D-sorbitol. The enzyme showed strong preference for NAD<sup>+</sup> but also displayed a very low yet detectable activity with NADP<sup>+</sup>. Mutational analysis of residue F59, the single

different substrate-binding residue between LADs and D-SDHs, failed to confer the enzyme the ability to accept D-sorbitol as a substrate, suggesting that the amino acids flanking the active site cleft may be responsible for the different activity and affinity patterns between LADs and SDHs. This enzyme should be useful for in vivo and in vitro production of xylitol and ethanol from L-arabinose.

**Keywords** Arabinose fermentation · Xylitol production · *N. crassa* genome · Alcohol dehydrogenase · Homology modeling · Ethanol production

**Electronic supplementary material** The online version of this article (doi:10.1007/s00253-007-1225-0) contains supplementary material, which is available to authorized users.

R. Sullivan · H. Zhao  
Department of Chemical and Biomolecular Engineering,  
University of Illinois at Urbana-Champaign,  
600 South Mathews Avenue,  
Urbana, IL 61801, USA

H. Zhao  
Department of Chemistry,  
University of Illinois at Urbana-Champaign,  
600 South Mathews Avenue,  
Urbana, IL 61801, USA

H. Zhao  
Center for Biophysics and Computational Biology,  
University of Illinois at Urbana-Champaign,  
600 South Mathews Avenue,  
Urbana, IL 61801, USA

H. Zhao (✉)  
Institute for Genomic Biology,  
University of Illinois at Urbana-Champaign,  
600 South Mathews Avenue,  
Urbana, IL 61801, USA  
e-mail: zhao5@uiuc.edu

## Introduction

Lignocellulosic biomass represents a renewable resource that is available in sufficient quantities from the corn wet-milling industry to serve as a low-cost feedstock (Saha and Bothast 1996). Some sources, particularly corn fiber, contain significant amounts of L-arabinose (Hespell 1998), an abundant pentose sugar second only to D-xylose in biomass composition. However, utilization of the L-arabinose content from hemicellulose hydrolysates for production of valued products has resulted in limited success. The inability of many yeasts and fungi to ferment L-arabinose appears to be a consequence of inefficient or incomplete assimilation pathways for this pentose sugar (McMillan and Boynton 1994). It has also been suggested that the cofactor imbalance necessary for the catabolism of L-arabinose also plays a factor (Verho et al. 2003). Recently, some progress has been made with the overexpression of either the bacterial utilization pathway (Becker and Boles 2003; Karhumaa et al. 2006) or the fungal pathway (Richard et al. 2003) for production of ethanol from L-arabinose. One benefit of utilizing the fungal pathway is that the intermediate xylitol is

also formed, which is a five-carbon sugar alcohol that has attracted much attention because of its potential as a natural food sweetener, a dental caries reducer, and a sugar substitute for diabetics (Saha and Bothast 1999).

L-Arabinitol 4-dehydrogenase (LAD, EC 1.1.1.12), a common enzyme found in yeasts and filamentous fungi, catalyzes the second step of the recently elucidated fungal L-arabinose metabolic pathway by oxidizing L-arabinitol to L-xylulose with concomitant NAD<sup>+</sup> reduction. LAD is purportedly a fungal orthologue of the eukaryotic sorbitol dehydrogenase (SDH; Pail et al. 2004) and belongs to the family of zinc-containing alcohol dehydrogenases. Several LADs have successfully been cloned and expressed (de Groot et al. 2005; Richard et al. 2001; Suzuki et al. 2005). However, they are not optimal for in vitro enzymatic production of xylitol because of their poor stability and/or activity.

In this paper, we report the cloning, heterologous expression, purification, and characterization of a new LAD from *Neurospora crassa*. In addition, based on sequence analysis and homology modeling, the single different substrate-binding residue F59 between LADs and SDHs was mutagenized. The resulting LAD variants failed to accept D-sorbitol as a substrate, suggesting that nonactive site residues in *N. crassa* LAD also play an important role in determining its substrate specificity. This enzyme is one of the most stable and active LADs ever reported.

## Materials and methods

**Materials** The *N. crassa* genomic sequence and LAD protein sequences were accessed from the National Center for Biotechnology Information ([www.ncbi.nlm.nih.gov](http://www.ncbi.nlm.nih.gov)). *N. crassa* 10333 was obtained from the American Type Culture Collection. *Escherichia coli* BL21(DE3), GST-Bind kit, biotinylated thrombin, and streptavidin agarose were purchased from Novagen (Madison, WI). *E. coli* WM1788 was kindly provided by William Metcalf at the University of Illinois (Urbana, IL). The glutathione *S*-transferase (GST) gene fusion expression vector pGEX-4T-3 was purchased from Amersham Biosciences (Piscataway, NJ). SuperScript™ One-Step reverse transcription polymerase chain reaction (RT-PCR) with Platinum® *Taq* kit was obtained from Invitrogen (Carlsbad, CA). Shrimp alkaline phosphatase and PCR grade deoxyribonucleotide triphosphates were obtained from Roche Applied Sciences (Indianapolis, IN). Phusion high-fidelity deoxyribonucleic acid (DNA) polymerase and DNA-modifying enzymes DNaseI, *EcoRI*, *NotI*, and T4 DNA ligase and their appropriate buffers were purchased from New England Biolabs (Beverly, MA). L-Arabinitol, D-arabinitol, adonitol, xylitol, D-sorbitol, D-mannitol, ampicillin, isopropyl-β-D-thiogalactopyranoside (IPTG), NADH,

NADP<sup>+</sup>, and NADPH were purchased from Sigma (St. Louis, MO). NAD<sup>+</sup> was a gift from Julich Fine Chemicals. Other required salts and reagents were purchased from Fisher (Pittsburgh, PA) or Sigma-Aldrich. The QIAprep spin plasmid mini-prep kit, QIAquick gel purification kit, RNeasy midiprep kit, and QIAquick PCR purification kit were purchased from Qiagen (Valencia, CA). Various oligonucleotide primers were obtained from Integrated DNA Technologies (Coralville, IA). Sodium dodecyl sulfate–polyacrylamide gel electrophoresis (SDS-PAGE) gel materials, electrophoresis equipment, protein size markers, size exclusion standards (catalog number 151–1901) and Bio-Sil SEC-250, 300×7.8 mm column were purchased from Bio-Rad (Hercules, CA).

**RT-PCR and cloning** *N. crassa* 10333 was grown on rich potato media at 30°C for 24 h and induced with 150 mM L-arabinose for 2 h. Because the predicted gene contained one intron, RT-PCR was utilized to isolate the processed gene. Total ribonucleic acid (RNA) was purified from collected cells (RNeasy purification kit, Qiagen) and treated with DNase I to remove residual genomic DNA. RT-PCR was performed using SuperScript™ One-Step RT-PCR with Platinum® *Taq* (Invitrogen) following the manufacturer's guidelines and suggestions for controls. The primers used for the RT-PCR were: forward 5'-GTA GCT ACG TCA **GAA TTC** CAT GGC TTC TAG CGC TTC C-3' and reverse 5'-GCT GAT TCT **GCG GCC GCT TAC** TCC AGA CTC TGG ATC-3'. The forward primer contained an *EcoRI* restriction site (shown in bold), while the reverse primer contained a *NotI* restriction site (shown in bold) and stop codon (italicized). The resulting RT-PCR product was isolated by a QIAquick agarose gel purification kit and amplified by an additional 20 cycles of PCR. The product was digested with *EcoRI* and *NotI* restriction enzymes and purified again by agarose gel electrophoresis. It was then ligated into pGEX-4T-3 which had been previously prepared by *EcoRI* and *NotI* digestion, dephosphorylation by shrimp alkaline phosphatase, and gel purification. The ligation mixture was precipitated with *n*-butanol and resuspended in water.

The new construct was used to transform *E. coli* WM1788 by electroporation. Positive clones were selected on Luria–Bertani (LB) solid media with ampicillin at 37°C overnight. All colonies were then removed from the plates and grown to saturation in 5 mL liquid LB from which the plasmids were purified using a QIAprep spin plasmid miniprep kit, which were used to transform *E. coli* BL21 (DE3) by heat shock. Positive clones were selected on LB solid media with ampicillin, picked individually, and assayed for LAD activity by the cell lysate assay described below. Plasmids were sequenced using the BigDye® Terminator sequencing method and an ABI PRISM 3700 sequencer (Applied Biosystems, Foster City, CA).

**Lysate assay** *E. coli* BL21 (DE3) harboring the pGEX-4T-3-derived vector were grown to a maximum optical density at 600 nm ( $OD_{600}$ ) at 37°C with shaking at 250 rpm. Fifty microliters was used to inoculate a new culture, which was grown at 37°C with shaking at 250 rpm until an  $OD_{600}$  of ~0.6 was reached. The cultures were then induced with 0.3 mM IPTG and shaken at 250 rpm at 25°C for 4 h. One milliliter of cells was harvested by centrifugation and lysed by resuspension in 1 mL of 1 mg/mL lysozyme/50 mM Tris (pH 8.0). The cells were frozen at –80°C and thawed at room temperature. The resulting lysate was vortexed thoroughly and centrifuged to remove cell debris. Ten microliters of the lysate was used in a kinetic assay with 200 mM L-arabinitol and 2 mM  $NAD^+$  as the substrates in 50 mM Tris (pH 8.0). To determine soluble and insoluble expression, lysozyme was utilized as the lysis reagent for the induced and normalized cells following the manufacturer's recommendations, and samples were subsequently analyzed by SDS-PAGE.

**GST-tag removal** The GST-tag was removed by incubation with biotinylated thrombin overnight at 4°C, incubation with streptavidin agarose for 30 min at 4°C to remove thrombin, and passing mixture through GST-Bind resin to remove GST-tag, leaving five residues (GlySerProAsnSer) attached to the N terminus of the *N. crassa* LAD sequence. To determine the effect of removal of the GST-tag, the purified LAD was incubated with and without thrombin at 4°C overnight. Complete cleavage of the 25.7 kDa tag was verified by SDS-PAGE. The specific activities of the cleaved and noncleaved samples were compared. It was determined that removal of the GST-tag enhanced activity by about 65%. Because of this significant difference in activity, the cleaved enzyme was used in all subsequent assays.

**Steady-state kinetics** Initial rates were determined by measuring the initial rate of reaction as observed by the increase of absorbance at 340 nm using a Varian Cary 100 Bio UV-visible spectrophotometer (Varian) at 25°C in 50 mM Tris (pH 8.0). Kinetic measurements with substrate and cofactor  $NAD^+$  were taken in a five-by-five matrix format, with substrate and cofactor concentrations varied from below their  $K_m$  to tenfold higher than their  $K_m$ . The kinetic data were analyzed with a modified version of Cleland's program (Cleland 1979).  $V_{max}$  and  $K_m$  for both substrate and  $NAD^+$  were obtained by fitting the data to a sequential ordered mechanism with  $NAD^+$  binding first, based on the proposed mechanism for SDH (Lindstad et al. 1992):

$$v = V_{max}AB / (K_{id}K_B + K_A B + K_B A + AB) \quad (1)$$

where  $v$  is the initial velocity,  $V_{max}$  is the maximum velocity,  $K_A$  and  $K_B$  are the Michaelis–Menten constants for  $NAD^+$  and substrate, respectively,  $A$  and  $B$  are the concentrations of  $NAD^+$  and substrate, respectively, and  $K_{id}$  is the dissociation constant for  $NAD^+$ . *N. crassa* LAD displayed typical Michaelis–Menten type kinetics with respect to all active substrates tested except D-sorbitol. The data represent averages of assays performed in duplicate or triplicate on two separate occasions.

**HPLC analysis** To determine the cofactor specificity of *N. crassa* LAD, 20  $\mu$ L reaction mixtures consisting of equal parts of 1 mM  $NAD(P)^+$  and 25 mM L-arabinitol in 50 mM Tris (pH 8.0) were set up, and following addition of approximately 1  $\mu$ g of enzyme, the reaction was allowed to proceed for 20 min at 37°C. Samples were eluted on a Zorbax 3.0 $\times$ 150 mm C-18 (3.5  $\mu$ m) column using an Agilent 1100 series high-performance liquid chromatography (HPLC) system equipped with a UV detector. The eluent consisted of two components: 0.1 M  $KH_2PO_4$  containing 5 mM tetrabutylammonium hydrogen sulfate (pH 5.5; buffer A) and 100% methanol (buffer B). The most suitable gradient was an initial isocratic step for 6 min at 93% buffer A, a gradient for 5 min from 7 to 30% buffer B, and a final isocratic step for 5 min at 30% buffer B. The quaternary structure of *N. crassa* LAD was determined using a Bio-Sil SEC-250 column (300 $\times$ 7.8 mm) and a mobile phase of 0.1 M  $Na_2HPO_4$ , 0.15 M NaCl, and 0.01 M  $NaN_3$ , pH 6.8.

**Metal analysis** Samples of thrombin-cleaved *N. crassa* LAD were buffer exchanged with 10 mM 4-(2-hydroxyethyl)piperazine-1-ethanesulfonic acid buffer (pH 8.0) and lyophilized. The identity and content of the metal were determined by inductively coupled plasma atomic emission spectrometry (OES Optima 2000 DV, Perkin Elmer, Boston, MA) in the Microanalytical Laboratory at the University of Illinois at Urbana-Champaign (Urbana, IL).

**Homology modeling** A homology model of *N. crassa* LAD was built using Insight II (Insight II, version 2000; Accelrys, San Diego, CA). The  $NAD^+$ -dependent human SDH (Protein Data Bank [PDB] accession code 1PL8; Pauly et al. 2003) and  $NADP^+$ -dependent SDH from silverleaf whitefly, *Bemisia argentifolii* (PDB accession code 1E3J; Banfield et al. 2001) were used as templates. The resulting model was docked with  $NAD^+$  and the catalytic zinc ion and subjected to energy minimization by using the Molecular Operating Environment (MOE, Chemical Computing Group, Montreal, Canada) program. To verify the model, the overall fold was checked using Profiles3-D (Insight II), and the allowed states for  $\phi$  and  $\psi$  angles and bond distances were checked using ProStat (Insight II), both with default settings.

## Results

*N. crassa* LAD gene identification LADs from *Hypocrea jecorina* (GenBank accession number AF355628.1) and *Aspergillus oryzae* (AB116938.2) were used as templates for a protein BLAST search ([www.ncbi.nlm.nih.gov](http://www.ncbi.nlm.nih.gov)). Utilizing the whole-genome sequence of *N. crassa* (Galagan et al. 2003), a postulated LAD-encoding gene, hypothetical protein NCU00643.1 (EAA36547.1), was discovered, which had the greatest sequence identity (~80%). This protein (referred to as *N. crassa* LAD hereafter) had a significant sequence identity (72 to 80% identity) with other LADs (Electronic supplementary material). Among the conserved residues were those that formed the active site and the structural Zn<sup>2+</sup>-binding site (Karlsson et al. 1995) and the glycine fingerprint (Lesk 1995) found in polyol dehydrogenases, as well as the majority of those shown to bind substrate in the SDH homologues (Pail et al. 2004).

*N. crassa* RNA purification, RT-PCR, cloning, and *N. crassa* LAD expression RT-PCR performed on total RNA isolated from L-arabinose-induced *N. crassa* 10333 showed the expected size of gene product. The RT-PCR product was cloned into the pGEX-4T-3 vector using *Eco*RI and *Not*I restriction sites and was transformed into *E. coli* BL21 (DE3). This construct (pGEX-lad1) expressed *N. crassa* LAD as an N-terminal GST-tagged fusion with a thrombin cleavage site. Cell lysates of IPTG-induced cultures of these cells were prepared, analyzed by SDS-PAGE, and assayed for LAD activities. The construct produced soluble GST-tagged *N. crassa* LAD at ~16% of the total soluble cellular proteins (Fig. 1), which was then purified in a single step with a GST-Bind kit according to manufacturer's protocol. The purified protein was desalted by ultrafiltration with several washes of 50 mM morpholinepropanesulfonic acid buffer (pH 7.25). After digesting with biotinylated thrombin, the enzyme was incubated with streptavidin agarose to remove the thrombin and then passed through GST-Bind resin again to remove the cleaved GST-tag. GST-tagged LAD cleaved with thrombin was used for characterization purposes, as it had about 65% greater specific activity than the tagged LAD enzyme. LAD stocks were stored frozen with 10% (v/v) glycerol at -80°C. Protein concentrations were determined by the Bradford method (Bradford 1976) and by using an estimated extinction coefficient (San Diego Supercomputer Center Biology Workbench [<http://workbench.sdsc.edu>]) of 35.3 mM<sup>-1</sup> cm<sup>-1</sup> at 280 nm with similar results. The purity of the protein was analyzed by an SDS-PAGE gel stained with Coomassie brilliant blue (Fig. 1). The final yield of protein was 30 mg/L of culture (~9 mg/g of *E. coli*) of greater than 95% pure LAD with a molecular mass of ~39 kDa, consistent with the predicted value of 39.6 kDa.

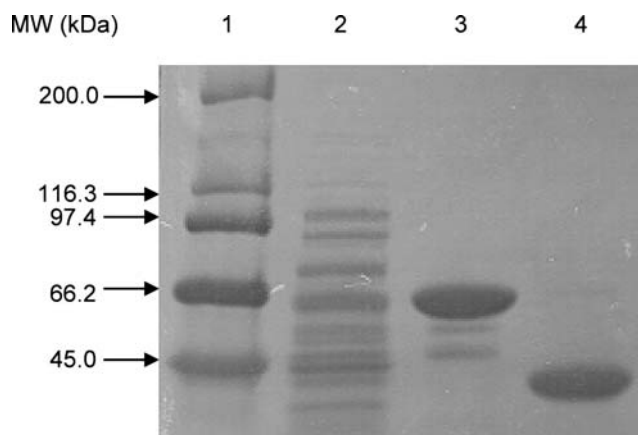


**Fig. 1** Overexpression and purification of recombinant *N. crassa* LAD. Lane 1, the molecular weight marker proteins (size in kDa is shown); lane 2, cell-free crude extract; lane 3, purified LAD enzyme with N-terminal GST-tag; lane 4, purified LAD enzyme with GST-tag removed by thrombin cleavage

*Steady-state kinetics* Purified *N. crassa* LAD displayed activity with NAD<sup>+</sup> as the preferred cofactor (Table 1), although there was small yet detectable activity with NADP<sup>+</sup>, which was verified by HPLC (see supplemental info). This is the first reported detection of NADP<sup>+</sup> utilization by LAD, although it is still considered a strongly NAD<sup>+</sup>-dependent enzyme.

Table 2 displays the kinetic constants of several other sugar alcohol substrates accepted by *N. crassa* LAD. D-Arabinitol, adonitol, xylitol, D-sorbitol, and D-mannitol were all examined as alternative substrates for *N. crassa* LAD with NAD<sup>+</sup> as the cofactor held at saturating concentration of 2 mM. Of the pentose sugar alcohols, only adonitol and xylitol acted as substrates, with *K<sub>m</sub>* values of 35 and 290 mM, respectively. This pattern of substrate promiscuity is similar to those of LADs isolated from other sources (Richard et al. 2001; Suzuki et al. 2005).

*Temperature dependence* The optimal temperature of activity was determined by assaying LAD activities at temperatures ranging from 12 to 65°C. The data show the optimum temperature to be between 45 and 55°C (Fig. 2a). At higher temperatures, the enzyme inactivates rapidly, and at lowered temperatures, the rate increases with temperature according to the Arrhenius equation. Utilizing the Arrhenius equation to fit the data from 12 to 30°C, the energy of activation for L-arabinitol oxidation by *N. crassa* LAD was determined to be 49 kJ/mol. The stability for *N. crassa* LAD was relatively high, as it retained activity at room temperature for longer than 1 month and at 4°C for several months. Thermal inactivation of *N. crassa* LAD was studied by incubating at 50°C in 50 mM Tris (pH 8.0), with samples removed at various times and assayed for activity in saturating substrate conditions. Figure 2b shows

**Table 1** Kinetic parameters for *N. crassa* LAD<sup>a</sup>

<i>N. crassa</i> LAD with indicated coenzyme	$K_m$ for NAD(P) (mean±SD) (μM)	$k_{cat}$ (mean±SD) (min <sup>-1</sup> )	$k_{cat}/K_m$ for NAD(P) (μM <sup>-1</sup> min <sup>-1</sup> )	$K_m$ for L-arabinitol (mean±SD) (mM)
NAD	174±24	1,206±54	6.9	16±3
NADP	–	–	$4.3 \times 10^{-5}$	–

<sup>a</sup> All assays were performed at 25 °C in 50 mM Tris, pH 8.0

the percentage of residual activity vs incubation time, which followed a first-order exponential decay with a half-life of 45 min. It is interesting to note that when tested at a slightly lower temperature of 45°C, the enzyme was able to retain ~60% of its activity after 4 h.

**pH rate profile** Enzyme activity was measured at pH values between 7.0 and 11.0 under saturating concentrations of NAD<sup>+</sup> (2 mM) and L-arabinitol (200 mM) in a universal buffer (50 mM morpholineethanesulfonic acid/50 mM Tris/50 mM glycine). The pH range for *N. crassa* LAD activity was large, with greater than 25% of the activity occurring with pH values of 7.0 to 11.0 (Fig. 2c). The pH optimum was around pH 9.5, and greater than 60% of the activity remained in the pH span from 8.0 to 10.5.

**Determination of mass and quaternary structure** Based on the standardized retention times of a Bio-Rad molecular mass standard, the molecular mass of LAD was calculated from its retention time to be ~152 kDa (Electronic supplementary material) using HPLC analysis. Monomerization was induced in the presence of 15% SDS, causing LAD to elute as a single peak with a retention time corresponding to a molecular mass of ~39 kDa. The data suggest that the native LAD is a noncovalently linked tetramer, which is typical for fungal-derived zinc-containing alcohol dehydrogenases (Korkhin et al. 1998).

**Metal analysis** *N. crassa* LAD was determined to contain very close to 2 mol of zinc/mol subunit. This is consistent with previously reported SDH and ADH enzymes containing both an active site zinc ion and a second zinc ion thought to be involved in stability (Banfield et al. 2001; Watanabe et al. 2005). The verification of the second zinc atom also correlates well with the four conserved cysteine

residues involved in structural zinc binding in homologous SDHs and xylitol dehydrogenases.

**Cofactor specificity** The cofactor specificity of *N. crassa* LAD was examined by HPLC. The separation of NAD<sup>+</sup>, NADP<sup>+</sup>, NADH, and NADPH was carried out as previously described (Woodyer et al. 2003). No discernible cross-contamination of oxidized cofactors was observed (data not shown). When NAD<sup>+</sup> was used as the cofactor, the products were analyzed by HPLC, and a single peak (UV 340 nm) was observed that had the same retention time as authentic NADH (Electronic supplementary material). The same process was carried out for NADP<sup>+</sup> as the cofactor, and a small yet detectable peak was observed with a retention time corresponding to an authentic sample of NADPH (Electronic supplementary material). This indicated the strong preference for NAD<sup>+</sup> as the cofactor of *N. crassa* LAD.

**Homology modeling** The structural model of *N. crassa* LAD was verified for consistency with known protein folds and allowed  $\psi$  and  $\phi$  angles. The Profiles3-D check resulted in a self-compatibility score of 139.94, which compares well to the scores of 150.53 and 145.49 for the coordinates from 1PL8 and 1E3J, respectively. The ProStat check of  $\phi$  and  $\psi$  angles were determined to be 81.2% within their core expected values, comparing well to the 83.3 and 82.4% for the same analysis of PDB structures 1PL8 and 1E3J, respectively.

This model was very similar to the human SDH crystal structure in overall fold and binding of coenzyme. The only major deviation between the backbone of these two structures is the N-terminal region of amino acids 1 through 8 (Fig. 3). However, this may be due to the different conformations of the N terminus between being in solution

**Table 2** Kinetic parameters for *N. crassa* LAD with other substrates<sup>a</sup>

<i>N. crassa</i> LAD with indicated substrate	$k_{cat}$ (mean±SD) (min <sup>-1</sup> )	$K_m$ (mean±SD) (mM)	$k_{cat}/K_m$ (mM <sup>-1</sup> min <sup>-1</sup> )	Percent activity
L-Arabinitol	1,210±30	18±2	67	100
Xylitol	970±40	290±27	3.3	4.9
Adonitol	1,080±30	35±3	31	46
D-Arabinitol	–	–	ND <sup>b</sup>	0
D-Sorbitol	– <sup>c</sup>	– <sup>c</sup>	– <sup>c</sup>	0 <sup>c</sup>
D-Mannitol	–	–	ND	0

<sup>a</sup> All assays were performed at 25°C in 50 mM Tris, pH 8.0, at saturated NAD<sup>+</sup> concentration

<sup>b</sup> ND Not detected

<sup>c</sup> Trace activity at 2 M D-sorbitol concentration, possibly because of substrate contamination

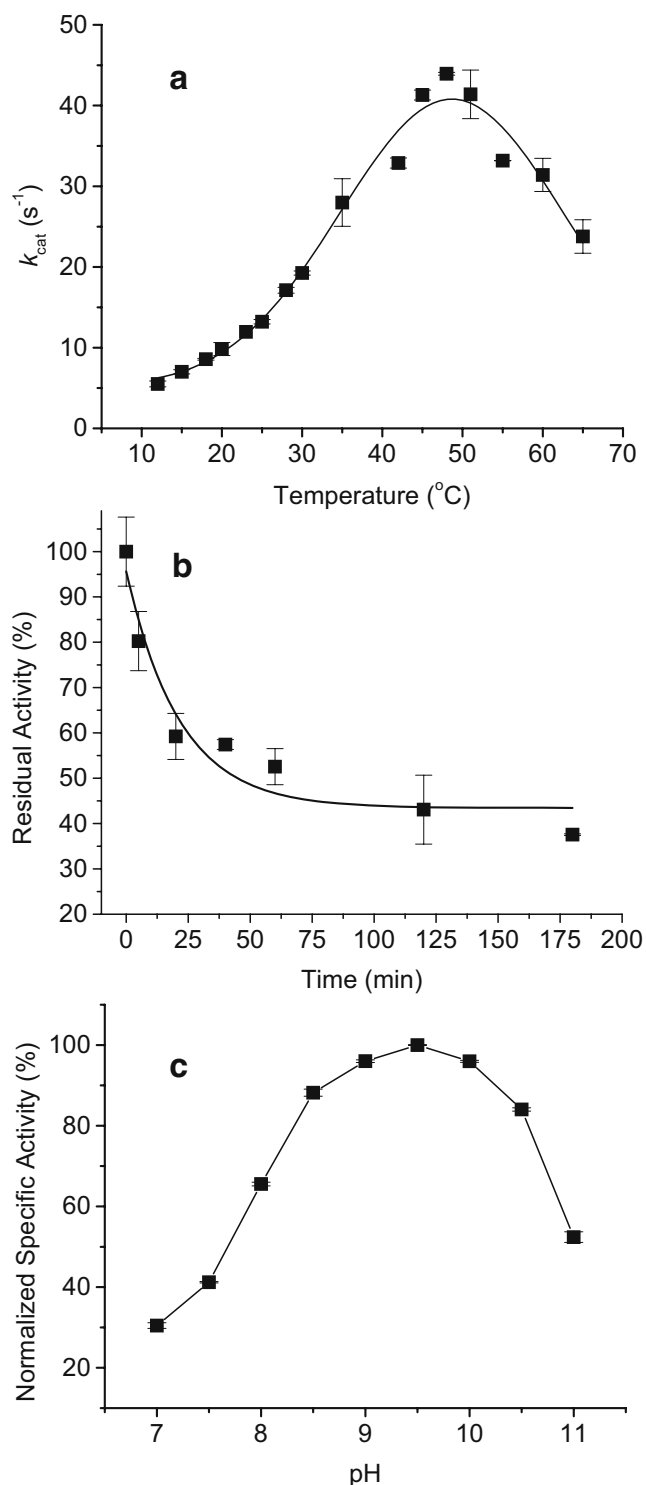


**Fig. 2** **a**  $k_{cat}$  dependence on temperature. *N. crassa* LAD was assayed at different temperatures from 12 to 65°C at saturating concentrations of 200 mM L-arabinitol and 2 mM NAD<sup>+</sup>. **b** Thermal inactivation of LAD at 50°C. The heat inactivation at 50°C was irreversible and followed first-order kinetics with a half-life of 45 min. **c** pH rate profile. Saturating concentrations of 200 mM L-arabinitol and 2 mM NAD<sup>+</sup> were used to measure the activity in a universal buffer at various pH values from 7.0 to 11.0

and forming dimerization contacts found to be present in SDH (Pauly et al. 2003). The conserved catalytic zinc-binding residues C53, H78, E79, and E163 have similar orientations and locations in the *N. crassa* LAD model (Fig. 3a). When comparing proposed substrate binding residues from SDH (Pail et al. 2004) to *N. crassa* LAD, the majority—S55, F127, T130, E163, R308, Y309—are strictly conserved and configured in similar orientations. However, one substrate-binding residue, F59, was different from the homologous tyrosine residue in SDH, making the *N. crassa* LAD-binding pocket slightly more hydrophobic (Fig. 3b).

**F59 mutant kinetic analysis** Enzyme activity assays were carried out for three mutants of *N. crassa* LAD (F59A, F59S, and F59Y) to study the effect of mutation of this active site, putative substrate-binding residue homologous to tyrosine in other SDHs. All assays were carried out similar to substrate specificity profile for the wild-type enzyme (see “Steady-state kinetics” in “Materials and methods”), with the cofactor NAD<sup>+</sup> held at saturating concentration of 2 mM for all assays. The mutants were still found to have activity with L-arabinitol, xylitol, and adonitol, and their kinetic parameters are displayed in Table 3. D-Sorbitol was also tested but showed no significant activity over the wild-type *N. crassa* LAD.

## Discussion

Hypothetical protein NCU00643.1 (EAA36547.1) from *N. crassa* was found to encode an LAD of 363 amino acid residues with a calculated  $M_r$  of 39,245. Sequence alignment with other reported LADs shows high homology (~70–80%), with conserved regions for Zn<sup>2+</sup> binding, cofactor binding, and active site residues. Comparison with several mammalian SDHs (mouse, rat, bovine, sheep, and human) showed ~40% homology, whereas comparison with xylitol dehydrogenases (*H. jecorina*, *A. oryzae*, *Candida tropicalis*, *Pichia stipitis*, and *Aspergillus fumigatus* Af293) was ~30% homology.

Kinetic parameters of characterized LADs from *H. jecorina*, *Aspergillus niger*, and *A. oryzae* are displayed in Table 4. It should be noted that only the LAD enzyme from *H. jecorina* by Pail et al. (2004) was purified to homogeneity, whereas the others were characterized either as partially purified enzymes (de Groot et al. 2005; Richard et al. 2001) or as cell-free extracts (Suzuki et al. 2005). The  $K_m$  value of *N. crassa* LAD was 16 mM for L-arabinitol, which when compared to LADs from *H. jecorina* and *A. niger*, is one of the lower values reported of characterized LADs. It should be noted, however, that values of 45

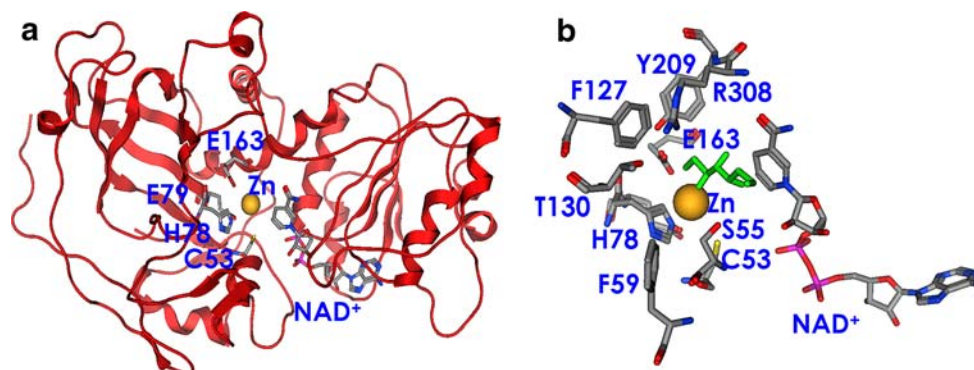


**Fig. 3** **a** Homology model of *N. crassa* LAD with bound  $\text{NAD}^+$  and catalytic zinc ion, built using the Insight II and MOE programs. The catalytic zinc ion ( $\text{Zn}^{2+}$ ), four catalytic zinc-binding residues, and  $\text{NAD}^+$  cofactor are colored by atom type. **b** Active site of *N. crassa*

LAD with docked catalytic zinc (shown in *space-fill*), cofactor  $\text{NAD}^+$ , and substrate L-arabinitol (colored green) coordinated with the active zinc. Key residues located within the substrate-binding pocket are labeled

(Richard et al. 2001) and 4.5 mM (Pail et al. 2004) were reported for the same *H. jecorina* LAD, although the enzymes were purified from different heterologous hosts (*S. cerevisiae* and *E. coli*, respectively), with the former LAD being obtained by cleavage of a GST-fusion protein. In addition, it is difficult to determine the effect of the larger  $K_m, \text{NAD}^+$  of *N. crassa* LAD compared to other LADs, as no other characterizations reported both  $k_{\text{cat}}$  and  $K_m$  values for the cofactor. With a specific activity of the purified *N. crassa* LAD equal to about 31 U/mg, it is almost 20-fold greater than *H. jecorina* LAD purified from *S. cerevisiae* heterologous expression and orders of magnitude higher than other LADs except for *A. niger* LAD, which shows about threefold greater specific activity than that of *N. crassa* LAD. However, it was also reported that the purified *A. niger* LAD was highly unstable, with rapidly diminishing activity at 4°C and complete loss of activity after freeze-thawing of the enzyme (de Groot et al. 2005). In

contrast, *N. crassa* LAD is quite stable and does not markedly lose activity when frozen repeatedly.

There has been no in-depth study of the substrate-binding residues for LAD, but the enzyme has been postulated to be a fungal orthologue of the eukaryotic D-SDHs (Pail et al. 2004), which have been investigated more thoroughly. Based on these reports, the active site substrate-binding residues are all strictly conserved in all LADs characterized to date (see [Electronic supplementary material](#) for sequence alignment analysis). When comparing these residues in *N. crassa* LAD to SDHs, only F59 was not conserved, which instead was a tyrosine residue in all of the SDHs examined. Mutational studies of this position were examined for F59A, F59S, and F59Y, to determine what effects this residue has on substrate specificity alteration, and are shown in Table 3. Replacement of the native F59 residue with the homologous tyrosine found in

**Table 3** Kinetic parameters of F59 mutants<sup>a</sup>

Substrate	Enzyme	$k_{\text{cat}}$ (mean±SD) ( $\text{min}^{-1}$ )	$K_m$ (mean±SD) (mM)	$k_{\text{cat}}/K_m$ ( $\text{mM}^{-1} \text{min}^{-1}$ )
L-Arabinitol	WT	1,210±30	18±2	67
	F59Y	840±30	42±5	20
	F59S	60±3	62±9	0.97
	F59A	— <sup>b</sup>	>400	0.12
Xylitol	WT	970±40	290±27	3.3
	F59Y	— <sup>b</sup>	>880	1.2
	F59S	— <sup>b</sup>	>1,400	0.04
	F59A	— <sup>b</sup>	>1,850	0.01
Adonitol	WT	1,080±30	35±3	31
	F59Y	1,420±50	193±11	7.4
	F59S	120±5	430±48	0.28
	F59A	— <sup>b</sup>	>1,110	0.03

<sup>a</sup> All assays were performed at 25°C in 50 mM Tris, pH 8.0.

<sup>b</sup> Saturation of substrate was not reached.

**Table 4** Kinetic parameters of LAD from various source organisms

Organism (reference)	Specific activity (U/mg)	$k_{\text{cat}}$ ( $\text{min}^{-1}$ )	$K_m, \text{L-arabinitol}$ (mM)	$k_{\text{cat}}/K_m, \text{L-arabinitol}$ ( $\text{mM}^{-1} \text{min}^{-1}$ )	$K_m, \text{NAD}^+$ ( $\mu\text{M}$ )
<i>N. crassa</i> (this work)	31	1,206	16	75	174
<i>H. jecorina</i> (Richard et al. 2001)	1.6	N/A <sup>a</sup>	40	N/A	180
<i>H. jecorina</i> (Pail et al. 2004)	0.013	51	4.5	11	N/A
<i>A. niger</i> (de Groot et al. 2005)	96	N/A	89	N/A	50
<i>A. oryzae</i> (Suzuki et al. 2005)	0.04	N/A	N/A	N/A	N/A

<sup>a</sup> N/A Not determined

SDH decreased the catalytic efficiency toward all active substrates. The ability of LAD to bind each substrate markedly decreased as the size of the amino acid at position 59 was decreased. Although these results suggest this residue is important for binding and catalysis for the active substrates of the wild-type LAD, it did not confer the enzyme the ability to accept D-sorbitol as a substrate. This confirms previously reported hypotheses that the amino acids flanking the active site cleft may be responsible for the activity and affinity patterns between LAD and SDH (Pail et al. 2004).

In summary, a gene from *N. crassa* encoding an LAD was cloned and purified. The enzyme is highly active and stable, acts on several five-carbon sugar alcohol substrates, and operates over a wide pH range. Mutational analysis indicates that nonactive site residues also play an important role in substrate specificity. This enzyme should prove useful in the production of xylitol and ethanol from L-arabinose derived from renewable resources.

**Acknowledgments** Support for this research was provided by Biotechnology Research and Development Consortium (BRDC; Project 2-4-121). Access to Insight II and MOE programs was provided by the University of Illinois School of Chemical Sciences' Computer Application and Network Services. We thank Nikhil Nair for his help with *N. crassa* growth and genomic DNA manipulation.

## References

- Banfield MJ, Salvucci ME, Baker EN, Smith CA (2001) Crystal structure of the NADP(H)-dependent ketose reductase from *Bemisia argentifolii* at 2.3 Å resolution. *J Mol Biol* 306:239–250
- Becker J, Boles E (2003) A modified *Saccharomyces cerevisiae* strain that consumes L-arabinose and produces ethanol. *Appl Environ Microbiol* 69:4144–4150
- Bradford MM (1976) A rapid and sensitive method for the quantitation of microgram quantities of protein utilizing the principle of protein-dye binding. *Anal Biochem* 72:248–254
- Cleland WW (1979) Statistical analysis of enzyme kinetic data. *Methods Enzymol* 63:103–38
- de Groot MJ, Prathumpai W, Visser J, Ruijter GJ (2005) Metabolic control analysis of *Aspergillus niger* L-arabinose catabolism. *Biotechnol Prog* 21:1610–1616
- Galagan JE, Calvo SE, Borkovich KA, Selker EU, Read ND, Jaffe D, FitzHugh W, Ma LJ, Smirnov S, Purcell S et al (2003) The genome sequence of the filamentous fungus *Neurospora crassa*. *Nature* 422:859–868
- Hespell R (1998) Extraction and characterization of hemicellulose from the corn fiber produced by corn wet-milling processes. *J Agric Food Chem* 46:2615–2619
- Karhumaa K, Wiedemann B, Hahn-Hagerdal B, Boles E, Gorwa-Grauslund MF (2006) Co-utilization of L-arabinose and D-xylose by laboratory and industrial *Saccharomyces cerevisiae* strains. *Microb Cell Fact* 5:18
- Karlsson C, Jornvall H, Hoog JO (1995) Zinc binding of alcohol and sorbitol dehydrogenases. *Adv Exp Med Biol* 372:397–406
- Korkhin Y, Kalb AJ, Peretz M, Bogin O, Burstein Y, Frolov F (1998) NADP-dependent bacterial alcohol dehydrogenases: crystal structure, cofactor-binding and cofactor specificity of the ADHs of *Clostridium beijerinckii* and *Thermoanaerobacter brockii*. *J Mol Biol* 278:967–981
- Lesk AM (1995) NAD-binding domains of dehydrogenases. *Curr Opin Struct Biol* 5:775–83
- Lindstad RI, Hermansen LF, McKinley-McKee JS (1992) The kinetic mechanism of sheep liver sorbitol dehydrogenase. *Eur J Biochem* 210:641–647
- McMillan JD, Boynton BL (1994) Arabinose utilization by xylose-fermenting yeasts and fungi. *Appl Biochem Biotechnol* 45–46:569–584
- Pail M, Peterbauer T, Seiboth B, Hametner C, Druzhinina I, Kubicek CP (2004) The metabolic role and evolution of L-arabinol 4-dehydrogenase of *Hypocrea jecorina*. *Eur J Biochem* 271:1864–1872
- Pauly TA, Ekstrom JL, Beebe DA, Chrunyk B, Cunningham D, Griffor M, Kamath A, Lee SE, Madura R, McGuire D et al (2003) X-ray crystallographic and kinetic studies of human sorbitol dehydrogenase. *Structure* 11:1071–1085
- Richard P, Londesborough J, Putkonen M, Kalkkinen N, Penttila M (2001) Cloning and expression of a fungal L-arabinol 4-dehydrogenase gene. *J Biol Chem* 276:40631–40637
- Richard P, Verho R, Putkonen M, Londesborough J, Penttila M (2003) Production of ethanol from L-arabinose by *Saccharomyces cerevisiae* containing a fungal L-arabinose pathway. *FEMS Yeast Res* 3:185–189
- Saha B, Bothast R (1996) Production of L-arabitol from L-arabinose by *Candida entomaeae* and *Pichia guilliermondii*. *Appl Microbiol Biotechnol* 45:299–306
- Saha B, Bothast R (1999) Production of xylitol by *Candida peltata*. *J Ind Microbiol Biotechnol* 22:633–636
- Suzuki T, Tran LH, Yogo M, Idota O, Kitamoto N, Kawai K, Takamizawa K (2005) Cloning and expression of NAD<sup>+</sup>-dependent L-arabinol 4-dehydrogenase gene (ladA) of *Aspergillus oryzae*. *J Biosci Bioeng* 100:472–474
- Verho R, Londesborough J, Penttila M, Richard P (2003) Engineering redox cofactor regeneration for improved pentose fermentation in *Saccharomyces cerevisiae*. *Appl Environ Microbiol* 69:5892–5897
- Watanabe S, Kodaki T, Makino K (2005) Complete reversal of coenzyme specificity of xylitol dehydrogenase and increase of thermostability by the introduction of structural zinc. *J Biol Chem* 280:10340–10349
- Woodyer R, van der Donk WA, Zhao H (2003) Relaxing the nicotinamide cofactor specificity of phosphite dehydrogenase by rational design. *Biochemistry* 42:11604–11614